Expression of indian hedgehog signaling in murine oviductal infundibulum and its relationship with epithelial homeostasis

Authors: Marina Hosotani[1*], Osamu Ichii[2, 3], Takashi Namba[2], Md. Abdul Masum[2], Teppei Nakamura[2, 4], Yasuhiro Hasegawa[5], Takafumi Watanabe[1], Yasuhiro Kon[2]

Addresses: [1]Laboratory of Veterinary Anatomy, School of Veterinary Medicine, Rakuno Gakuen University, Ebetsu, Hokkaido 069-8501, Japan

[2]Laboratory of Anatomy, Department of Basic Veterinary Science, Faculty of Veterinary Medicine, Hokkaido University, Sapporo, Hokkaido 060-0818, Japan

[3]Laboratory of Agrobiomedical Science, Faculty of Agriculture, Hokkaido University, Sapporo, Hokkaido 060-0818, Japan

[4]Department of Biological Safety Research, Chitose Laboratory, Japan Food Research Laboratories, Chitose, Hokkaido 066-0052, Japan

[5]Department of Food Science and Human Wellness, College of Agriculture, Food and Environment Science, Rakuno Gakuen University, Ebetsu, Japan

[*]**Corresponding author: Marina Hosotani, DVM,**

Laboratory of Veterinary Anatomy, School of Veterinary Medicine, Rakuno Gakuen University, Midorimachi 582, Bunkyodai, Ebetsu 069-8501, Japan

19 Tel & Fax: +81-11-388-4763

20 Email: m-hosotani@rakuno.ac.jp

21

22 **Acknowledgements and Funding Information**

23 This work was supported in part by JSPS KAKENHI Grant (No. 19K23708 and 21K05976),

24 Rakuno Gakuen University Research Fund (No. 2020-01), Suhara Memorial Foundation Research

25 Grants, and Uehara Memorial Foundation Research Incentives Grants (M. H.). The research

26 described in this paper was presented in part and awarded at the 163rd Japanese Association of

27 Veterinary Anatomists, 14-30 September 2020, online.

Abstract

Homeostasis of the oviductal infundibulum epithelium is continuously regulated by signaling pathways under physiological and pathological conditions. Herein, we investigated the expression of hedgehog (Hh) signaling-related components in the murine oviductal infundibulum, which is known to maintain homeostasis in the adult epithelium. Additionally, using autoimmune disease-prone MRL/MpJ-Fas$^{lpr/lpr}$ (MRL/lpr) mice showing abnormal morphofunction of the ciliated epithelium of the infundibulum related to the oviductal inflammation, we examined the relationship between Hh signaling and pathology of the infundibulum. The expression and localization of Pax8, a marker for progenitor cells in the oviductal epithelium, and Foxj1, a marker for ciliogenesis, were examined in the infundibulum. The results showed that Pax8 was downregulated and Foxj1 was upregulated with aging, suggesting that homeostasis of the infundibulum epithelium of MRL/lpr mice was disturbed at 6 months of age. In all mice, the motile cilia of ciliated epithelial cells in the infundibulum harbored Hh signaling pathway-related molecules: patched (Ptch), smoothened (Smo), and epithelial cells harbor Gli. In contrast, *Ptch*, *Smo*, and *Gli2* were significantly downregulated in the infundibulum of MRL/lpr mice at 6 months of age. The expression levels of *Pax8* and *Foxj1* were significantly positively correlated with those of *Ptch1*, *Smo*, and *Gli2*. Hh signaling is thought to be involved in homeostasis of the ciliated epithelium in the infundibulum. In MRL/lpr mice, which show exacerbated severe systemic

autoimmune abnormalities, molecular alterations in Hh signaling-related components are considered to interact with local inflammation in the infundibulum, leading to disturbances in epithelial homeostasis and reproductive function.

Keywords: autoimmune abnormality, ciliated epithelium, hedgehog signaling pathway, homeostasis, oviduct

Introduction

Mammalian oviducts are divided into three parts, the infundibulum, ampulla, and isthmus, in order from the distal to proximal parts. The different composition ratios of ciliated epithelial cells and secretory cells in the epithelium of each part reflect the unique reproductive function in each section (Li et al. 2017; Koyama et al. 2019). Particularly, the infundibulum epithelium is composed mostly of ciliated epithelial cells, so that ciliary beating effectively moves oocytes produced in the ovaries into the oviductal lumen; this process is known as oocyte pick-up. Oocyte pick-up and transportation are disturbed by abnormal ciliary morphofunction in the infundibulum caused by pathological conditions such as smoking (Talbot and Riveles 2005), hormonal dysregulation (Raidt et al. 2015), and inflammation (Hosotani et al. 2020). Physiologically, the proportion of ciliated epithelial cells and secretory cells in the infundibulum epithelium changes under hormonal dynamics through the estrous cycle (Ito et al. 2016). In addition, the infundibulum is constantly exposed to follicular fluid containing inflammatory molecules during each ovulation, which damages the ciliary epithelium (Palma-Vera et al. 2017). Therefore, the infundibulum epithelium continuously undergoes epithelial turnover to maintain its healthy histology and reproductive function under both physiological and pathological conditions.

Adult epithelial homeostasis is maintained by the proliferation and differentiation of epithelial stem cells, which are regulated by activation of signaling pathways such as the Wnt/β-catenin,

70 Notch, and Hedgehog (Hh) signaling pathways (Sancho et al. 2004; Carlier et al. 2020). In
71 oviductal epithelial homeostasis, secretory cells act as progenitors by self-renewing and/or
72 differentiating into ciliated epithelial cells (Ghosh et al. 2017). The molecular mechanism
73 underlying these effects is not fully understood; however, several studies have focused on the
74 involvement of Wnt/β-catenin signaling (Ghosh et al. 2017) and Notch signaling (Zhu et al. 2019)
75 in homeostasis of the oviductal epithelium. In contrast, although homeostasis of the adult tracheal
76 ciliated epithelium is maintained by activation of the Hh signaling pathway (Peng et al. 2015), the
77 involvement of this pathway in maintaining the oviductal epithelium has not been explored.
78 In a murine model of systemic autoimmune disease, MRL/MpJ-Fas$^{lpr/lpr}$ (MRL/lpr) mice
79 develop severe inflammation of the lamina propria in the oviductal infundibulum. Chronic
80 abnormal immune conditions result in abnormal morphofunction in the ciliated epithelium, such
81 as decreased numbers of ciliated epithelial cells, elongation of the cilia, and disorientation of ciliary
82 beating (Hosotani et al. 2018, 2020). These pathological conditions are closely related to
83 disturbances in epithelial homeostasis but the underlying molecular mechanism is unclear.
84 In this study, we investigated expression of the Hh signaling pathway in the murine
85 infundibulum epithelium and its relationship with homeostasis of the infundibulum epithelium. In
86 addition, we examined the expression of Hh signaling pathway-related molecules in MRL/lpr mice
87 as a destruction model of the infundibulum epithelium and compared the results with those

88 obtained the healthy infundibulum of C57BL/6N mice (B6) as a general strain and MRL/MpJ mice

89 (MRL/+) as wild-type MRL/lpr mice.

Material and methods

Animals

Animal experiments were approved by the School of Veterinary Medicine, Rakuno Gakuen University (approval no. VH19A6). The animals were handled in accordance with the Guide for the Care and Use of Laboratory Animals, Rakuno Gakuen University, Japan. Female B6, MRL/+, and MRL/lpr mice at 3 and 6 months of age were obtained from Japan SLC, Inc. (Hamamatsu, Shizuoka, Japan). Previous studies reported that autoimmune disease is severely exacerbated in female MRL/lpr mice at 6 months of age compared to at 3 months of age (Hosotani et al. 2018, 2020). The mice were housed in groups within plastic cages at 18–26°C under a 12-h light/dark cycle and had free access to a commercial diet and water. The estrous cycle of each mouse under the natural estrous cycle was confirmed by monitoring vaginal smears (Byers et al. 2012). All mice were euthanized by either severing the carotid artery or cervical dislocation under deep anesthesia using a mixture of medetomidine (0.3 mg/kg), midazolam (4 mg/kg), and butorphanol (5 mg/kg). The spleen was collected from the mice and weighed as a marker of autoimmune disease.

Immunostaining

Mouse female reproductive organs were collected and fixed with 4% paraformaldehyde at 4°C overnight, embedded in paraffin, and cut into 3-µm-thick sections, which were then used for

immunohistochemistry (IHC) and immunofluorescence (IF). Detailed information on the antibodies, antigen retrieval, and serum blocking is listed in Table 1. The sections were incubated in 20 mM Tris-HCl (pH 9.0) for 15 min at 110°C, 10 mM citrate buffer (pH 6.0) for 15 min at 110°C, or 0.1% pepsin for 5 min at 37°C. The sections for IHC were soaked in methanol containing 0.3% hydrogen peroxide. Sections incubated with blocking serum for 60 min at room temperature were incubated overnight at 4°C with primary antibodies. Negative controls were performed with normal mouse IgG (sc-2025, Santa Cruz Biotechnology Inc., Santa Cruz, CA, USA), normal rat IgG (sc-2026, Santa Cruz Biotechnology) and normal rabbit IgG (sc-2027, Santa Cruz Biotechnology). After three washes in 0.01 M PBS, the sections were incubated with secondary antibodies for 30 min and washed. The sections for IHC were incubated for 30 min at room temperature, using a streptavidin-biotin complex (SABPRO Kit, Nichirei, Tokyo, Japan), and then incubated with 3,3′-diaminobenzidine tetrahydrochloride-hydrogen peroxide solution, and lightly stained with hematoxylin. The stained sections of the outer infundibulum were examined using a BZ-X710 microscope (Keyence, Osaka, Japan).

Three semi-serial sections stained with IHC for detection of Foxj1 with 50-μm intervals were used, and the percentage of expelled non-ciliated epithelial cells and the percentage of Foxj1 positive expelled non-ciliated epithelial cells were calculated as follows, respectively: percentage of expelled non-ciliated epithelial cells (%) = 100 × number of expelled non-ciliated epithelial

126 cells / number of total 80-100 epithelial cells in the field. Percentage of Foxj1 positive expelled
127 non-ciliated epithelial cells (%) = 100 × number of Foxj1 positive expelled non-ciliated epithelial
128 cells / number of total 10-20 expelled non-ciliated epithelial cells in the field.
129
130 ***Reverse Transcription and Quantitative Real-time Polymerase Chain Reaction***
131 The oviducts were manually separated into the proximal (including the isthmus and ampulla)
132 and distal (including infundibulum) parts and homogenized using a BioMasher (Nippi Inc., Tokyo,
133 Japan). Total RNA was purified using the NucleoSpin® RNA Plus kit (Macherey-Nagel, Düren,
134 Germany) according to the manufacturer's instructions. The purified total RNA was used as a
135 template to synthesize cDNA using ReverTra Ace qPCR RT Master Mix (Toyobo Co., Ltd., Osaka,
136 Japan). Quantitative real-time polymerase chain reaction (qPCR) analysis of the cDNA was
137 performed using THUNDERBIRD SYBR qPCR Mix (Toyobo Co., Ltd.) and gene-specific
138 primers (Table 2, Sigma-Aldrich, St. Louis, MO, USA). The qPCR cycling conditions were 95°C
139 for 1 min, followed by 40 cycles of 95°C for 15 s and 52°C or 60°C for 45 s. Data were normalized
140 against the expression level of actin, beta (*Actb*) and analyzed using the ΔCt method to compare
141 the expression of genes encoding hedgehog ligands; the ΔΔCt method was used to compare the
142 expression of other genes.
143

144 ***In Situ Hybridization***

145 Paraformaldehyde-fixed paraffin-embedded specimens of female reproductive organs were
146 cut into 5μm-thick sections, air-dried overnight, and baked in an oven for 60 min at 60°C. RNA *in*
147 *situ* hybridization was performed using an RNAscope® 2.5 HD Detection Regent-Brown kit
148 (Advanced Cell Diagnostics, Newark, CA, USA) according to the manufacturer's instructions. The
149 RNAscope® positive control probe-Mm-Polr2a (Cat. No. 312471, Advanced Cell Diagnostics),
150 RNAscope® negative control probe-DapB (Cat. No. 310043, Advanced Cell Diagnostics),
151 RNAscope® probe-Mm-Shh (Cat. No. 314361, Advanced Cell Diagnostics), RNAscope® probe-
152 Mm-Dhh (Cat. No. 415031, Advanced Cell Diagnostics), and RNAscope® probe-Mm-Ihh-noXHs
153 (Cat. No. 413091, Advanced Cell Diagnostics) were used.

154

155 ***Statistical Analysis***

156 The results are expressed as the mean ± standard error (s.e.). Data among three or more groups
157 were compared using Tukey's test ($P < 0.05$). Data between two groups were compared using
158 Student's *t*-test ($P < 0.05$). Correlations between two parameters were analyzed using Spearman's
159 correlation test ($P < 0.05$). Statistical analysis was conducted using JMP 14.2.0 (SAS Institute, Inc.,
160 Cary, NC, USA).

Result

Expression and Localization of Epithelial Homeostasis-Related Molecules in the Infundibulum

In the oviductal epithelium, Pax8 is a marker of secretory cells (i.e., progenitor cells), whereas Foxj1 is a marker of ciliogenesis. Pax8 was localized in the nucleus of secretory cells in the infundibulum of mice, except for in MRL/lpr mice at 6 months of age (Figure 1a-c and a'-c'). Foxj1 was localized in the nucleus of ciliated epithelial cells in the infundibulum of mice, except for MRL/lpr mice at 6 months of age, in which Foxj1 expression was observed not only in the nucleus of ciliated epithelial cells as well as that of non-ciliated epithelial cells expelled from the epithelium (Figure 1d-f and d'-f'). There was no significant differences in the percentage of expelled non-ciliated epithelial cells composing the infundibulum epithelium among the strains and ages (Figure 1h), while the percentage of Foxj1 positive expelled non-ciliated epithelial cells was significantly higher in MRL/lpr mice at 6 months of age than other strains and MRL/lpr mice at 3 months of age (Figure 1i).

We compared the transcriptional expression levels of *Pax8* and *Foxj1* in the infundibulum as the distal part of the oviduct with those in the ampulla and isthmus as the proximal part (Figure 2a and b). *Pax8* expression was lower in the distal part than in the proximal part of all strains at 3 months of age. In the entire oviduct of MRL/lpr mice at 6 months of age, *Pax8* expression showed an age-related decrease and was significantly lower than that in the other strains. In contrast, *Foxj1*

179 expression was higher in the distal part than in the proximal part of all mice. In the entire oviduct
180 of MRL/lpr, *Foxj1* expression was higher than in other strains, particularly at the distal part which
181 showed a significant age-related increase.
182
183 ***Expression and Localization of Hedgehog Signaling-Related Molecules in Infundibulum***
184 The canonical Hh signaling pathway in primary cilia is activated by binding of Hh ligands such
185 as sonic, indian, and desert Hh (Shh, Ihh, and Dhh, respectively) to the transmembrane protein
186 patched (Ptch), followed by an interaction with smoothened (Smo) and the activation of GLI
187 family zinc finger 1–3 (Gli1–3) transcription factors (Briscoe and Thérond 2013). There were no
188 significant differences in the expression of Hh signaling pathway-related genes during the estrous
189 cycle (Figure 4a-e); therefore, we focused on the infundibulum of mice at estrus. In all mice, Ptch1
190 and Smo were localized in the cilia of ciliated epithelial cells in the infundibulum (Figure 3a-a’’’’,
191 b-b’’’’, c-c’’’’, d-d’’’’, e-e’’’’, and f-f’’’’). The fluorescence intensity of Ptch1 and Smo in the
192 infundibulum did not differ between mice of different strains and ages. In B6 and MRL/+ mice,
193 Gli2 was highly expressed in the nucleus of secretory cells and faintly in the nucleus of ciliated
194 epithelial cells in the infundibulum (Figure 3g-g’’’’, h-h’’’’). In MRL/lpr mice at both 3 and 6
195 months of age, Gli2 was ubiquitously observed in the nuclei of cells comprising the infundibulum
196 epithelium (Figure 3i-i’’’’).

197 In transcriptional analysis, *Ptch1* expression did not significantly differ among the oviductal
198 parts of all mice (Figure 5a). *Ptch1* expression showed an age-related decrease in the proximal part
199 of B6 and at both the proximal and distal parts in MRL/lpr mice. In the entire oviduct of MRL/lpr
200 mice, *Ptch1* expression was significantly lower than that in B6 or/and MRL/+ mice. *Smo*
201 expression was significantly higher in the distal part than in the proximal part of B6 and MRL/+
202 mice at 3 months of age (Figure 5b). *Smo* expression showed an age-related decrease at the distal
203 part in all mice. In the entire oviduct of MRL/lpr, *Smo* expression was significantly lower than that
204 in the other strains. *Gli1* expression was significantly lower at the distal part than at the proximal
205 part: *Gli2* and *Gli3* expression showed no significant differences among the oviductal parts (Figure
206 5c-e). In the entire oviduct of MRL/lpr, *Gli1* expression showed an age-related decrease and was
207 significantly lower than that in the other strains (Figure 5c). The mean C_t value of Gli1 expression
208 in the distal parts was high above around 32 in all mice (data not shown), so that the localization
209 level of Gli1 protein seems to be very low in the distal part. In the entire oviduct of MRL/lpr, *Gli2*
210 expression was significantly higher than in other strains, particularly at the distal part at 6 months
211 of age (Figure 5d). *Gli3* expression tended to be higher in the entire oviduct of MRL/lpr mice at 3
212 months of age than in other strains, whereas that of MRL/lpr at 6 months of age showed an age-
213 related decrease and was significantly lower than that in other strains (Figure 5e).

214 Among the transcription factors of the hedgehog ligands (*Shh*, *Dhh*, and *Ihh)*, *Shh* and *Dhh*

were not expressed in the infundibulum epithelium or ovarian granulosa cells (Figure 6a-f and a'-f'), whereas *Ihh* was highly expressed in ovarian granulosa cells and slightly in infundibulum epithelial cells (Figure 6a''-f''). *Ihh* expression in ovarian granulosa cells was lower in MRL/lpr mice than in B6 mice (Figure 6a'' and e''). The *Shh* and *Dhh* expression levels were not significantly different among the oviductal parts, whereas *Ihh* expression was lower in the distal part than in the proximal part in all mice (Figure 7a-f).

Relation between Hh Signaling Pathway and Oviductal Epithelial Homeostasis

Correlation analysis of transcriptional expression in the oviduct of mice at 3 months of age was performed (Table 3). In the proximal part, *Ptch1* and *Pax8* expression was significantly positively correlated with the expression of all Hh signaling pathway-related genes. *Foxj1* expression showed the same results, except for *Gli1*. In contrast, at the distal part, *Ptch1* expression was significantly positively correlated with the expression of *Smo* and *Gli2* and significantly negatively correlated with *Gli3* expression. *Pax8* and *Foxj1* expression was significantly positively correlated with the expression of *Ptch1*, *Smo*, and *Gli2*.

Discussion

The molecular mechanism that maintains homeostasis of the infundibulum epithelium has been greatly altered in autoimmune disease model mice. This molecular alteration causes an abnormal morphology of the ciliated epithelium of the infundibulum of MRL/lpr mice at 6 months of age, such as a decreased proportion of ciliated epithelial cells, elongated cilia, and disorientation of ciliary alignment (Hosotani et al. 2020). The transcription factor Pax8 governs the expression of a series of genes pivotal to tissue development in thyroid follicular cells and Müllerian ducts (Plachov et al. 1990; Grote et al. 2006). Pax8 in the oviductal secretory cells is a marker of the self-renewal and differentiation of these cells to ciliated epithelial cells (Ghosh et al. 2017); therefore, the significant downregulation of Pax8 transcripts and proteins suggests that Pax8 attenuates epithelial homeostasis in the infundibulum of MRL/lpr at 6 months of age. The transcription factor Foxj1 is required for the late steps of ciliogenesis, including docking of centrioles at the apical membrane to form basal bodies and axoneme elongation (You et al. 2004). Foxj1 upregulation promotes abnormal ciliogenesis, resulting in disorganized, dense, and lengthened cilia in the airway ciliated cells of patients with chronic mucosal inflammation (Li et al. 2014). Considering that the direction of coordinated ciliary beating requires basal body polarization (Kunimoto et al. 2012), in the infundibulum of MRL/lpr mice at 6 months of age, significant upregulation of Foxj1 may promote abnormal ciliogenesis, resulting in cilia elongation

248 and disoriented ciliary alignment. Foxj1 localization in the expelled non-ciliated epithelial cells
249 was significantly observed in the infundibulum of MRL/lpr mice at 6 months of age, which implies
250 the increase of inadequate ciliogenesis and the promoted elimination of epithelial cells failed to
251 differentiate to ciliated epithelial cells. Otherwise, significantly high expression of Foxj1 may have
252 been a reaction to the decreased number of ciliated epithelial cells following disturbed ciliogenesis
253 and loss of $Pax8^{+}$ epithelial progenitor cells. The abnormal morphofunction of the ciliated
254 epithelium of the infundibulum caused by alterations in homeostasis-related molecules causes
255 dysfunction in oocyte pick-up (Hosotani et al. 2018, 2020).

256 This study revealed that the motile cilia of ciliated epithelial cells in the infundibulum harbor
257 Hh signaling pathway-related molecules: the transmembrane receptors, Ptch and transmembrane
258 protein adjacent to Ptch, and Smo (Carpenter et al. 1998). In addition, Hh signaling effectors in
259 the Gli family are expressed in the nucleus of infundibulum epithelial cells. Considering the
260 significant positive correlations between Ptch1 and Smo/Gli2 in the infundibulum, motile cilia in
261 the infundibulum epithelium contain the Hh signaling pathway, although whether this pathway is
262 canonical or non-canonical matter has not been determined. Although primary cilia (i.e., immotile
263 cilia) are generally considered as sensor cilia in which canonical/non-canonical Hh signaling is
264 transduced (Abou Alaiwi et al. 2009; Bangs and Anderson 2017), recent studies reported that
265 motile cilia also act as sensors of the pericellular environment. The motile cilia of the tracheal

epithelium express sensing receptors such as the bitter taste receptor and Ptch1/Smo (Shah et al. 2009; Nordgren et al. 2014), which sense injury and chronic inflammation in the airway. The motile cilia in oviducts harbor progesterone receptors, which regulate the ciliary beat frequency (Teilmann et al. 2006; Bylander et al. 2010). Thus, motile cilia in the infundibulum epithelium may play a sensing role via Hh signaling-related components. Hh ligands were not significantly expressed in the infundibulum, and the present and previous studies (Russell et al. 2007) revealed Ihh expression in ovarian granulosa cells, where Hh signaling may induce granulosa cell proliferation. Therefore, cilia in the infundibulum may receive Ihh produced by ovarian granulosa cells at the time of ovulation, rather than through the paracrine effect of Hh produced by infundibulum epithelial cells.

In the infundibulum, *Pax8* and *Foxj1* expression showed a significant positive correlation with the gene expression of Hh signaling pathway-related *Ptch1*, *Smo*, and *Gli2*. This suggests that the Hh signaling pathway is closely related to the regulation of epithelial homeostasis in the infundibulum. To the best of our knowledge, direct molecular interactions between Pax8 and/or Foxj1 and the Hh signaling pathway during development and homeostasis maintenance have not been observed previously. However, Pax8 has been predicted as a target gene activated via the Shh signaling pathway in oncogenesis (Harter et al. 2015). During the development of central nervous system, Foxj1 expression is regulated by the Shh signaling pathway and alters the response of cells

to Shh signaling (Cruz et al. 2010). Although further studies are needed to determine the molecular relationship between Pax8, Foxj1, and Hh signaling-related components, the significant downregulation of the Ptch1 and Smo transcripts in the infundibulum of MRL/lpr mice at 6 months of age may be related to the abnormal pathology of the ciliated epithelium. The alternation of Gli2 localization in the infundibulum of MRL/lpr mice compared to other strains would relate to the downregulation of Ptch1 and Smo transcripts and the disruption of Hh signaling

Aged MRL/lpr mice show autoimmune disease-prone phenotypes in systemic organs, including the oviductal infundibulum with infiltration of autoreactive immune cells because of a mutation in the Fas cell surface death receptor (*Fas*) gene (Andrews et al. 1978; Watanabe-Fukunaga et al. 1992; Hosotani et al. 2020). MRL/lpr at 3 months of age showed expression of *Ptch1*, *Smo*, and *Gli1-3* in the infundibulum, and thus specific genetic alterations in the MRL/lpr strain do not cause significant downregulation of Hh signaling-related components. In contrast, alterations in Hh signaling transduction were reported to trigger immunological modulation. In the skin of atopic dermatitis mouse models and the central nervous system with autoimmune neuroinflammation, Shh signaling suppresses immune reactions via T-regulatory cell signaling and reduces tissue pathology and disease severity (Papaioannou et al. 2019; Benallegue et al. 2021). In adult intestinal mesenchyme, Shh and Ihh act as anti-inflammatory epithelial modulators and modulate tolerogenic versus proinflammatory signaling (Zacharias et al. 2010). Therefore, significant

downregulation of *Ptch1* and *Smo* transcripts may interact with severe autoimmune inflammation in the oviductal lamina propria of MRL/lpr mice at 6 months of age (Hosotani et al. 2020). Furthermore, the deteriorated supply of fresh Hh signaling-related components in the infundibulum of MRL/lpr mice at 6 months of age may be related to abnormal homeostasis of the ciliated epithelium. The damages on ciliary morphofunction caused by variations in levels of inflammatory cytokines in the infundibulum of MRL/lpr mice (Hosotani et al. 2020) are thought to reflect the physiological damage of ciliated epithelium of infundibulum caused by inflammatory follicular fluid (Palma-Vera et al. 2017), in terms of inflammatory cytokines altering the morphofunction of the ciliated epithelium of infundibulum. Therefore, the downregulation of Hh signaling-related components caused by the inflammatory molecules would also relate to the turnover of the infundibulum epithelium under physiological conditions.

We observed a difference in the molecular expression between the infundibulum and ampulla/isthmus. Epithelial cells in the distal and proximal parts of the oviducts are from intrinsically different lineages and are maintained separately (Ford et al. 2020). The properties and populations of $Pax8^+$ epithelial cells differ between the distal and proximal parts; the infundibulum shows a low population of $Pax8^+$ secretory cells (Ford et al. 2020). Foxj1 upregulation in the infundibulum compared to in the proximal part reflects greater activation of ciliogenesis and a larger population of ciliated epithelial cells in the infundibulum. Hh signaling-related components

were transcribed in the proximal part, despite the sparse presence of cilia. In contrast, correlation analysis indicated that Gli1 is involved in Hh signaling in the proximal part and that Gli1 and Gli3 are involved in epithelial homeostasis. Further investigations are required to reveal the effects of the difference in molecular expression patterns among oviductal parts.

In summary, we propose the different mechanism of Hh signaling transduction between in healthy and autoimmune disease conditions (Figure 8a and b). We propose that homeostasis of ciliated epithelium in the infundibulum is regulated not only by Wnt/β-catenin and Notch signaling, but also possibly by Hh signaling. In addition, alterations in Hh signal transduction related to the abnormal immune condition in the oviduct of MRL/lpr disrupts the epithelial morphology in the infundibulum, resulting in oocyte pick-up dysfunction. Further functional study on the change of the epithelial morphology in infundibulum under the experimental manipulation of Hh signaling would strengthen the role of Hh signaling in the epithelial homeostasis in oviducts. Our results improve the understanding of the physiology and pathology of mammalian female reproductive function.

Author contributions

Conceptualization: M.H. and O.I.; Methodology: M.H., O.I., Ta.N., M.A.M, Te.N. and Y. H.; Validation: M.H., O.I., and T.N.; formal analysis: M.H. and O.I.; Investigation: M.H., O.I., Ta.N. and M.A.M.; Resources: M.H., O.I., and M.A.M.; Data curation: M.H.; Writing - original draft: M.H. and O.I.; Writing - review & editing: M.H., O.I., T.W., and Y.K.; Visualization: M.H. and O.I.; Supervision: M.H. and Y.K.; Project administration: O.I. and YK; Funding acquisition: M.H.

Conflicts of interest

The authors declare no conflicts of interest.

Ethical approval

Animal experimentation was approved by the School of Veterinary Medicine, Rakuno Gakuen University (approval no. VH19A6). Animals were handled in accordance with the Guide for the Care and Use of Laboratory Animals, Rakuno Gakuen University, Japan.

Data, material, and/or code availability

The data that support the findings of this study are available from the corresponding author upon reasonable request.

References

Abou Alaiwi WAA, Lo ST, Nauli SM (2009) Primary cilia: Highly sophisticated biological sensors. Sensors (Basel) 9:7003–7020

Andrews BS, Eisenberg RA, Theofilopoulos AN, et al (1978) Spontaneous murine lupus-like syndromes. Clinical and immunopathological manifestations in several strains. J Exp Med 148:1198–1215

Bangs F, Anderson KV (2017) Primary cilia and Mammalian Hedgehog signaling. Cold Spring Harb Perspect Biol 9. https://doi.org/10.1101/cshperspect.a028175

Benallegue N, Kebir H, Kapoor R, et al (2021) The hedgehog pathway suppresses neuropathogenesis in CD4 T cell-driven inflammation. Brain 144:1670–1683. https://doi.org/10.1093/brain/awab083

Briscoe J, Thérond PP (2013) The mechanisms of Hedgehog signalling and its roles in development and disease. Nat Rev Mol Cell Biol 14:416–429

Byers SL, Wiles M V., Dunn SL, Taft RA (2012) Mouse estrous cycle identification tool and images. PLoS One 7:e35538. https://doi.org/10.1371/JOURNAL.PONE.0035538

Bylander A, Nutu M, Wellander R, et al (2010) Rapid effects of progesterone on ciliary beat frequency in the mouse Fallopian tube. Reprod Biol Endocrinol 8:48. https://doi.org/10.1186/1477-7827-8-48

Carlier FM, Dupasquier S, Ambroise J, et al (2020) Canonical WNT pathway is activated in the airway epithelium in chronic obstructive pulmonary disease. EBiomedicine 61. https://doi.org/10.1016/j.ebiom.2020.103034:103034

Carpenter D, Stone DM, Brush J, et al (1998) Characterization of two patched receptors for the vertebrate hedgehog protein family. Proc Natl Acad Sci U S A 95:13630–13634. https://doi.org/10.1073/pnas.95.23.13630

Cruz C, Ribes V, Kutejova E, et al (2010) Foxj1 regulates floor plate cilia architecture and modifies the response of cells to sonic hedgehog signalling. Development 137:4271–4282. https://doi.org/10.1242/dev.051714

Ford MJ, Harwalkar K, Pacis AS, et al (2021) Oviduct epithelial cells constitute two developmentally distinct lineages that are spatially separated along the distal-proximal axis. Cell Rep 36:109677. https://doi.org/10.1101/2020.08.21.261016

Ghosh A, Syed SM, Tanwar PS (2017) In vivo genetic cell lineage tracing reveals that oviductal secretory cells self-renew and give rise to ciliated cells. Development 144:3031–3041. https://doi.org/10.1242/dev.149989

Grote D, Souabni A, Busslinger M, Bouchard M (2006) Pax2/8-regulated Gata3 expression is necessary for morphogenesis and guidance of the nephric duct in the developing kidney. Development 133:53–61. https://doi.org/10.1242/dev.02184

Harter PN, Baumgarten P, Zinke J, et al (2015) Paired box gene 8 (PAX8) expression is associated with sonic hedgehog (SHH)/wingless int (WNT) subtypes, desmoplastic histology and patient survival in human medulloblastomas. Neuropathol Appl Neurobiol 41:165–179. https://doi.org/10.1111/nan.12186

Hosotani M, Ichii O, Nakamura T, et al (2018) Autoimmune abnormality affects ovulation and oocyte-pick-up in MRL/MpJ-Fas lpr/lpr mice. Lupus 27:82–94. https://doi.org/10.1177/0961203317711772

Hosotani M, Ichii O, Nakamura T, et al (2020) Altered ciliary morphofunction in the oviductal infundibulum of systemic autoimmune disease-prone MRL/MpJ-Fas lpr/lpr mice. Cell Tissue Res 380:627–641. https://doi.org/10.1007/s00441-020-03175-z

Ito S, Kobayashi Y, Yamamoto Y, et al (2016) Remodeling of bovine oviductal epithelium by mitosis of secretory cells. Cell Tissue Res 366:403–410. https://doi.org/10.1007/s00441-016-2432-8

Koyama H, Shi D, Fujimori T (2019) Biophysics in oviduct: Planar cell polarity, cilia, epithelial fold and tube morphogenesis, egg dynamics. Biophys Physicobiol 16:89–107. https://doi.org/10.2142/biophysico.16.0_89

Kunimoto K, Yamazaki Y, Nishida T, et al (2012) Coordinated ciliary beating requires Odf2-mediated polarization of basal bodies via basal feet. Cell 148:189–200.

https://doi.org/10.1016/j.cell.2011.10.052

Li S, O'Neill SRS, Zhang Y, et al (2017) Estrogen receptor α is required for oviductal transport of embryos. FASEB J 31:1595–1607. https://doi.org/10.1096/fj.201601128R

Li YY, Li CW, Chao SS, et al (2014) Impairment of cilia architecture and ciliogenesis in hyperplastic nasal epithelium from nasal polyps. J Allergy Clin Immunol 134:1282–1292. https://doi.org/10.1016/j.jaci.2014.07.038

Nordgren TM, Wyatt TA, Sweeter J, et al (2014) Motile cilia harbor serum response factor as a mechanism of environment sensing and injury response in the airway. Am J Physiol Lung Cell Mol Physiol 306:L829–L839

Palma-Vera SE, Schoen J, Chen S (2017) Periovulatory follicular fluid levels of estradiol trigger inflammatory and DNA damage responses in oviduct epithelial cells. PLOS ONE 12:e0172192. https://doi.org/10.1371/journal.pone.0172192

Papaioannou E, Yánez DC, Ross S, et al (2019) Sonic Hedgehog signaling limits atopic dermatitis via Gli2-driven immune regulation. J Clin Invest 129:3153–3170. https://doi.org/10.1172/JCI125170

Peng T, Frank DB, Kadzik RS, et al (2015) Hedgehog actively maintains adult lung quiescence and regulates repair and regeneration. Nature 526:578–582. https://doi.org/10.1038/nature14984

424 Plachov D, Chowdhury K, Walther C, et al (1990) Pax8, a murine paired box gene expressed in
425 the developing excretory system and thyroid gland. Development 110:643–651
426 Raidt J, Werner C, Menchen T, et al (2015) Ciliary function and motor protein composition of
427 human fallopian tubes. Hum Reprod 30:2871–2880. https://doi.org/10.1093/humrep/dev227
428 Russell MC, Cowan RG, Harman RM, et al (2007) The hedgehog signaling pathway in the
429 mouse ovary. Biol Reprod 77:226–236. https://doi.org/10.1095/biolreprod.106.053629
430 Sancho E, Batlle E, Clevers H (2004) Signaling pathways in intestinal development and cancer.
431 Annu Rev Cell Dev Biol 20:695–723
432 Shah AS, Ben-Shahar Y, Moninger TO, et al (2009) Motile cilia of human airway epithelia are
433 chemosensory. Science 325:1131–1134. https://doi.org/10.1126/science.1173869
434 Talbot P, Riveles K (2005) Smoking and reproduction: The oviduct as a target of cigarette
435 smoke. Reprod Biol Endocrinol 3:52. https://doi.org/10.1186/1477-7827-3-52
436 Teilmann SC, Clement CA, Thorup J, et al (2006) Expression and localization of the
437 progesterone receptor in mouse and human reproductive organs. J Endocrinol 191:525–535.
438 https://doi.org/10.1677/joe.1.06565
439 Watanabe-Fukunaga R, Brannan CI, Copeland NG, et al (1992) Lymphoproliferation disorder in
440 mice explained by defects in Fas antigen that mediates apoptosis. Nature 356:314–317.
441 https://doi.org/10.1038/356314a0, 1372394

442 You Y, Huang T, Richer EJ, et al (2004) Role of f-box factor foxj1 in differentiation of ciliated
443 airway epithelial cells. Am J Physiol Lung Cell Mol Physiol 286:L650–L657.
444 https://doi.org/10.1152/ajplung.00170.2003
445 Zacharias WJ, Li X, Madison BB, et al (2010) Hedgehog is an anti-inflammatory epithelial
446 signal for the intestinal lamina propria. Gastroenterology 138:2368–77, 2377.e1.
447 https://doi.org/10.1053/j.gastro.2010.02.057
448 Zhu M, Iwano T, Takeda S (2019) Estrogen and EGFR pathways regulate Notch signaling in
449 opposing directions for multi-ciliogenesis in the Fallopian tube. Cells 8:933
450 https://doi.org/10.3390/cells8080933

FIGURE LEGENDS

Fig. 1 Localization of Pax8 and Foxj1 in the oviductal infundibulum. IHC of Pax8 (a-c and a'-c'), Foxj1 (d-f and d'-f'), and negative control (g) are shown. Bar = 25 μm. Black arrows: immunoreactive positive epithelial cells; red arrowheads: expelled non-ciliated epithelial cells from the epithelium. (h) The percentage of expelled non-ciliated epithelial cells from the epithelium in distal parts of oviducts. There were no significant differences between ages at the same strains (Student's t-test, $P < 0.05$) and among strains at the same age (Tukey's test, $P < 0.05$). (i) The percentage of Foxj1 positive expelled non-ciliated epithelial cells from the epithelium distal parts of oviducts. *: Significant differences between 3 and 6 months of age at the same strains and same part (Student's *t*-test, $P < 0.05$). B&M: Significant differences between B6 or MRL/+ mice at the same age (Tukey's test, $P < 0.05$). B6 = C57BL/6N, MRL/+ = MRL/MpJ, MRL/lpr = MRL/MpJ-*Fas*$^{lpr/lpr}$

Fig. 2 Expression levels of *Pax8* (a) and *Foxj1* (b) in the oviduct. Data are the mean ± s.e. *: Significant differences between 3 and 6 months of age at the same strains and same part (Student's *t*-test, $P < 0.05$). #: Significant differences between proximal and distal parts of oviducts from mice of the same strains and age (Student's *t*-test, $P < 0.05$). B&M: Significant differences between B6 or MRL/+ mice at the same age (Tukey's test, $P < 0.05$). *Pax8*: Paired box 8; *Foxj1*: Forkhead box

protein J1. B6 = C57BL/6N, MRL/+ = MRL/MpJ, MRL/lpr = MRL/MpJ-*Fas*$^{lpr/lpr}$

Fig. 3 Localization of hedgehog signaling-related proteins in the oviductal infundibulum revealed by immunofluorescence. Localization of Ptch1 (a-a’’’’, b-b’’’’, and c-c’’’’), Smo (d-d’’’’, e-e’’’’, and f-f’’’’), Gli2 (g-g’’’’, h-h’’’’, and i-i’’’’), and negative control (j-j’’) are shown. Bar = 25 μm. Arrows: immunoreactive positive cells in the epithelium. B6 = C57BL/6N, MRL/+ = MRL/MpJ, MRL/lpr = MRL/MpJ-*Fas*$^{lpr/lpr}$

Fig. 4 Expression levels during estrous cycle of hedgehog signaling-related genes in the oviduct of C57BL/6N at 3 months of age. Expression levels of *Ptch1* (a), *Smo* (b), *Gli1* (c), *Gli2* (d), and *Gli3* (e) are shown. Data are the mean ± s.e. *: Significant differences between 3 and 6 months of age at the same cycle and same part (Student’s *t*-test, $P < 0.05$). #: Significant differences between proximal and distal parts of oviducts from mice of the same cycle and age (Student’s *t*-test, $P < 0.05$). There were no significant differences among estrous cycles at the same age and part (Tukey’s test, $P < 0.05$). P: proximal part; D: distal part 3m: 3 months of age, 6m: 6 months of age. *Ptch1*: Patched-1, *Smo*: Smoothened, *Gli1-3*: GLI family zinc finger 1–3.

Fig. 5 Expression levels of hedgehog signaling-related genes in the oviduct. Expression levels of

Ptch1 (a), *Smo* (b), *Gli1* (c), *Gli2* (d), and *Gli3* (e) are shown. Data are the mean ± s.e. *: Significant differences between 3 and 6 months of age for the same strains and same part (Student's *t*-test, $P < 0.05$). #: Significant differences between proximal and distal parts of oviducts from mice of the same strains and age (Student's *t*-test, $P < 0.05$). B&M: Significant differences between B6 or MRL/+ mice at the same age (Tukey's test, $P < 0.05$). *Ptch1*: Patched-1, *Smo*: Smoothened, *Gli1-3*: GLI family zinc finger 1-3. B6 = C57BL/6N, MRL/+ = MRL/MpJ, MRL/lpr = MRL/MpJ-*Fas*$^{lpr/lpr}$

Fig. 6 Expression of transcriptions of hedgehog in ovarian granulosa cells (a-a'', c-c'', and e-e'') and epithelial cells of the oviductal infundibulum (b-b'', d-d'', and f-f'') revealed by *in situ* hybridization. Negative controls are shown in (g and g'). Brown dots indicate positive reactions to *in situ* hybridization. Bar = 25 μm. Arrows: reaction-positive cells in the oviductal infundibulum. B6 = C57BL/6N; MRL/lpr = MRL/MpJ-*Fas*$^{lpr/lpr}$

Fig. 7 Expression levels of hedgehog genes in the oviduct of B6 at 3 months of age (a and d), MRL/+ at 3 months of age (b and e), and MRL/lpr at 3 months of age (c and f). Data are the mean ± s.e. *: Significant differences between proximal and distal parts of oviducts from mice of the same strains and age (Student's *t*-test, $P < 0.05$). 3: Significant differences between 3 and 6 months

505 of age in mice of the same strains and from the same part (Student's *t*-test, $P < 0.05$). B&M:
506 Significant differences between B6 or MRL/+ mice at the same age (Tukey's test, $P < 0.05$). B6 =
507 C57BL/6N, MRL/+ = MRL/MpJ, MRL/lpr = MRL/MpJ-*Fas*$^{lpr/lpr}$
508
509 **Fig. 8** Estimated modulation mechanisms of hedgehog signaling in the oviductal infundibulum
510 between healthy (a and a') and autoimmune disease conditions (b and b'). In healthy condition,
511 hedgehog signaling transduced by Ihh released by the ovarian granulosa cells, which is received
512 by Ptch1 and Smo localized on the motile cilia of the oviductal infundibulum. The hedgehog
513 signaling mediated by Ptch1, Smo, and Gli2 in the ciliated epithelial cells would lead the constant
514 transcription and protein production of Ptch1 and Smo and maintain the proliferation of Pax8
515 positive secretory cells and differentiation of those into Foxj1 positive healthy ciliated epithelial
516 cells in the oviductal infundibulum. In autoimmune disease condition, the declined levels of Ihh
517 production and transcription of Ptch1 and Smo causes the modulation of hedgehog signaling
518 transduction, which resulted in the disturbances in the homeostasis of ciliated epithelium of the
519 oviductal infundibulum and the appearance of strongly Foxj1 positive ciliated epithelial cells
520 which are morphologically abnormal. CEC: ciliated epithelial cell, SC: secretory cell, NCEC: non
521 ciliated epithelial cell, GCs: granulosa cells, Foxj1: forkhead box J1, Pax8: paired box 8, Hh:
522 Hedgehog, Ihh: indian hedgehog, Ptch1: Patched-1, Smo: Smoothened, Gli2: GLI family zinc

finger 2.

524 **Table 1. Primary antibody information in immunostaining.**

Antigen	Cat. No	Source	Host	Dilution	Antigen retrieval reagent	Blocking serum	Secondary antibody for IF (1:300)	Biotinylated secondary antibody for IHC
Gli2	NBP2-23602	Novus Biologicals LLC., Littleton, CO, USA	Rabbit	1:200	20 mM tris-HCl (pH 9.0)	10% goat normal serum	Goat anti-rabbit IgG H&L CF568, 20103-1 (Biotium.Inc, Hayward, CA)	-
Ptch1	MAB41051	R&D Systems Inc., Minneapolis, MN, USA	Rat	1:200	0.1% pepsin	10% goat normal serum	Goat anti-rat IgG H&L CF568, 20096-1 (Biotium.Inc, Hayward, CA)	-
Smo	GTX60154	GeneTex Inc., Irvine, CA, USA	Rabbit	1:200	0.1% pepsin	10% goat normal serum	Goat anti-rabbit IgG H&L CF568, 20103-1 (Biotium.Inc, Hayward, CA)	-
Tubulin-α	MS-581-R7	Thermo Scientific, Waltham,	Mouse	Undiluted	No need	10% goat normal serum	Goat anti-mouse IgG H&L CF488A, 20018-1 (Biotium.Inc, Hayward, CA)	-

		MA, USA						
Foxj1	14-9965-80	Invitrogen, Carlsbad, CA, USA	Mouse	1:500	10 mM citrate buffer (pH 6.0)	10% rabbit normal serum	-	Rabbit anti-mouse IgG+IgA+IgM antibody, 426031, undiluted (Nichirei, Tokyo, Japan)
Pax8	ACR438A	Biocare Medical, Pacheco, CA, USA	Mouse	1:100	20 mM tris-HCl (pH 9.0)	10% rabbit normal serum	-	Rabbit anti-mouse IgG+IgA+IgM antibody, 426031, undiluted (Nichirei, Tokyo, Japan)

525 IF: immunofluorescence, IHC: immunohistochemistry.

526 **Table 2. Primer list used for quantitative PCR analysis.**

Genes	Accession Number	Primer Sequence (5′-3′) F: Forward, R: Reverse	Product size (bp)	Annealing temp. (℃)
Actb	NM_007393.5	F: TGTTACCAACTGGGACGACA R: GGGGTGTTGAAGGTCTCAAA	165	60
Dhh	NM_007857.5	F: TTGGCACTCTTGGCACTATCT R: CTTTGCAACGCTCTGTCATC	277	60
Foxj1	NM_008240.3	F: ACTATGCCACCAACCCACA R: GGATGGAATTCTGCCAGGT	171	60
Gli1	NM_010296.2	F: CGACCTGCAAACCGTAATC R: CTTGCCAACCATCATATCCA	289	60
Gli2	NM_001081125.1	F: TGGAGAAGAAAGAAGCCAAGAG R: TCATGTCAATCGGCAAAGG	159	60
Gli3	NM_008130.3	F: CCTGCTCCAACATTTCCAAC R: CTTGACTAGGGTTGTTCCTTCC	240	60

Ihh	NM_010544.3	F: CCTCTTGCCTACAAGCAGTTC R: AGATGGCCAGTGAGTTCAGAC	214	60
Pax8	NM_011040.4	F: AAGCATCGACTCACAGAGCA R: GAATGAGGATCTGCCACCAC	285	60
Ptch1	NM_001328514.1	F: CCATGACAAAGCCGACTACA R: GGAAGACTGCGCACACTAGAA	293	60
Shh	NM_009170.3	F: CAAGTACGGCATGCTGGCTC R: AAGGTGAGGAAGTCGCTGTA	254	52
Smo	NM_176996.4	F: GTCTCTGCACGCTCTTCACA R: CCAGACTACTCCAGCCATCAA	269	60

Dhh: desert hedgehog, *Foxj1*: forkhead box J1, *Gli1-3*: GLI family zinc finger 1–3, *Ihh*: Indian hedgehog, *Pax8*: paired box 8, *Ptch1*: Patched 1, *Shh*: sonic hedgehog, *Smo*: smoothened, frizzled class receptor.

Table 3. Spearman's correlation coefficient (ρ) between hedgehog signaling-related genes expression and secretory/ciliated epithelial cells marker expression in the oviduct of mice at 3 months of age.

		Parameters					
		Hedgehog receptor gene expression	Secretory and ciliated epithelial cells marker expression		Hedgehog receptor gene expression	Secretory and ciliated epithelial cells marker expression	
		at proximal part			at distal part		
		Ptch1	*Pax8*	*Foxj1*	*Ptch1*	*Pax8*	*Foxj1*
Ptch1	ρ	1	**0.55*** **	**0.38** **	1	**0.63*** **	**0.62*** **
	P	-	**<0.0001**	**0.0071**	-	**<0.0001**	**<0.0001**
Smo	ρ	**0.60*** **	**0.62*** **	**0.42** **	**0.48*** **	**0.48*** **	**0.59*** **
	P	**<0.0001**	**<0.0001**	**0.0026**	**0.0007**	**0.0007**	**<0.0001**
Gli1	ρ	**0.63*** **	**0.49*** **	0.20	0.19	0.13	0.23
	P	**<0.0001**	**0.0005**	0.1690	0.1981	0.3862	0.1226
Gli2	ρ	**0.56*** **	**0.72*** **	**0.69*** **	**0.43** **	**0.61*** **	**0.69*** **

	P	**<0.0001**	**<0.0001**	**<0.0001**	**0.0027**	**<0.0001**	**<0.0001**
Gli3	ρ	**0.41****	**0.39****	**0.35***	**-0.30***	-0.09	0.07
	P	**0.0038**	**0.0059**	**0.0141**	**0.0431**	0.5554	0.6623

Ptch1, Patched-1; *Smo*, Smoothened; *Gli1-3*, GLI family zinc finger 1–3, *Pax8*, paired box 8; *Foxj1*, forkhead box J1.

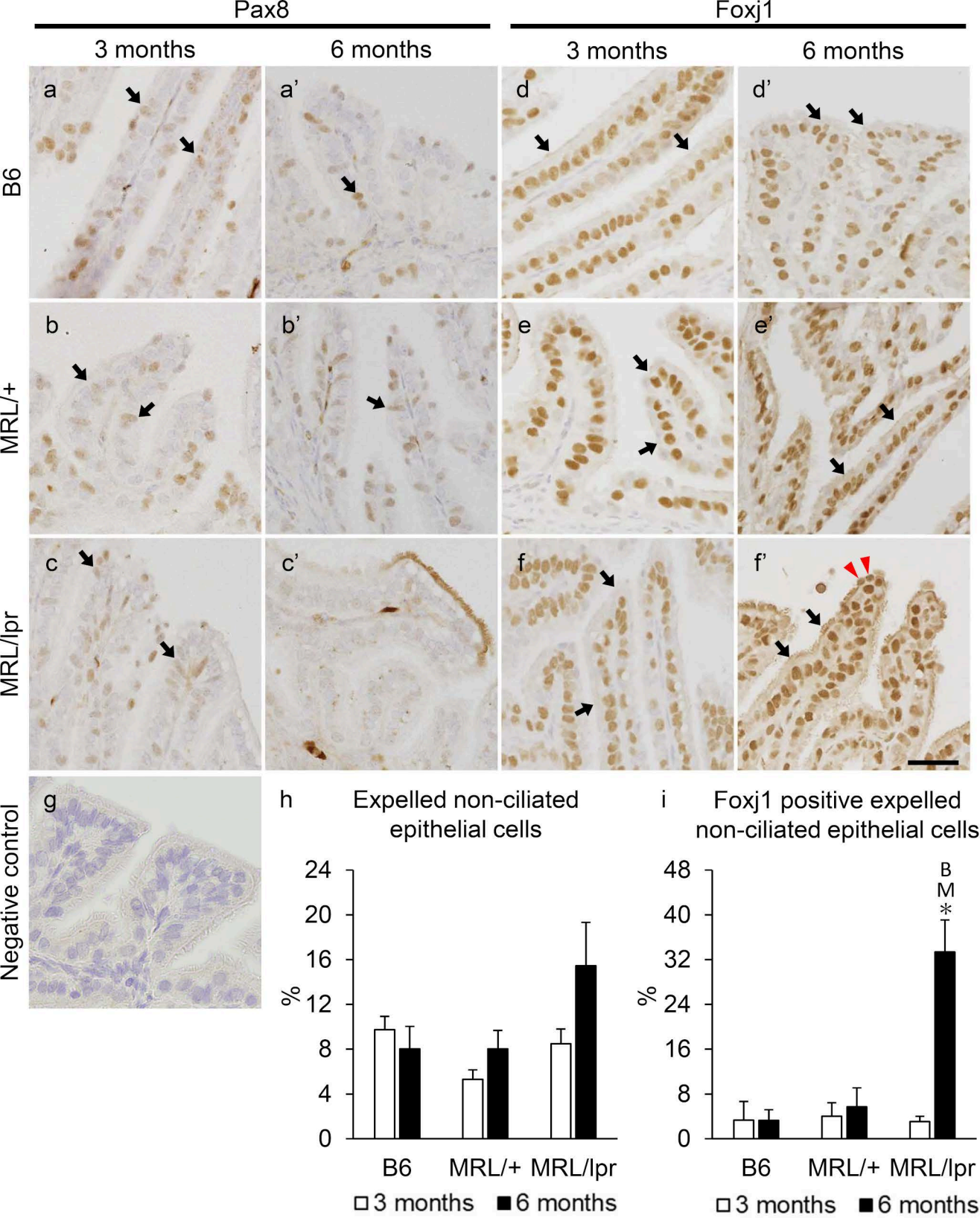
Pax8
Foxj1
3 months
6 months
3 months
6 months
B6
MRL/+
MRL/lpr
Negative control
a
a'
d
d'
b
b'
e
e'
c
c'
f
f'
g
h
Expelled non-ciliated epithelial cells
%
24
20
16
12
8
4
0
B6
MRL/+
MRL/lpr
3 months
6 months
i
Foxj1 positive expelled non-ciliated epithelial cells
%
48
40
32
24
16
8
0
B
M
*
B6
MRL/+
MRL/lpr
3 months
6 months

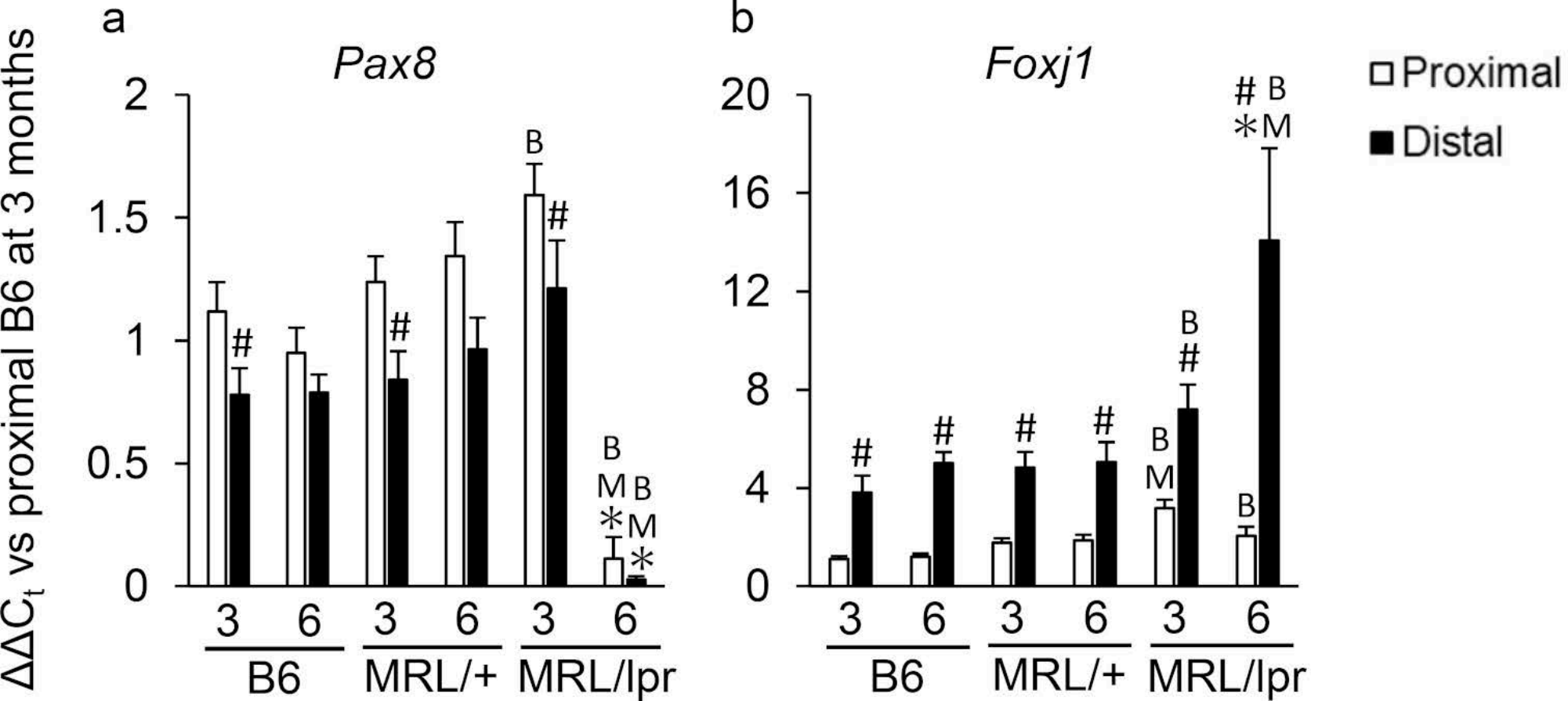
a
Pax8
b
Foxj1
Proximal
Distal
ΔΔCt vs proximal B6 at 3 months
2
1.5
1
0.5
0
20
16
12
8
4
0
3
6
B6
MRL/+
MRL/lpr
#
*
B
M

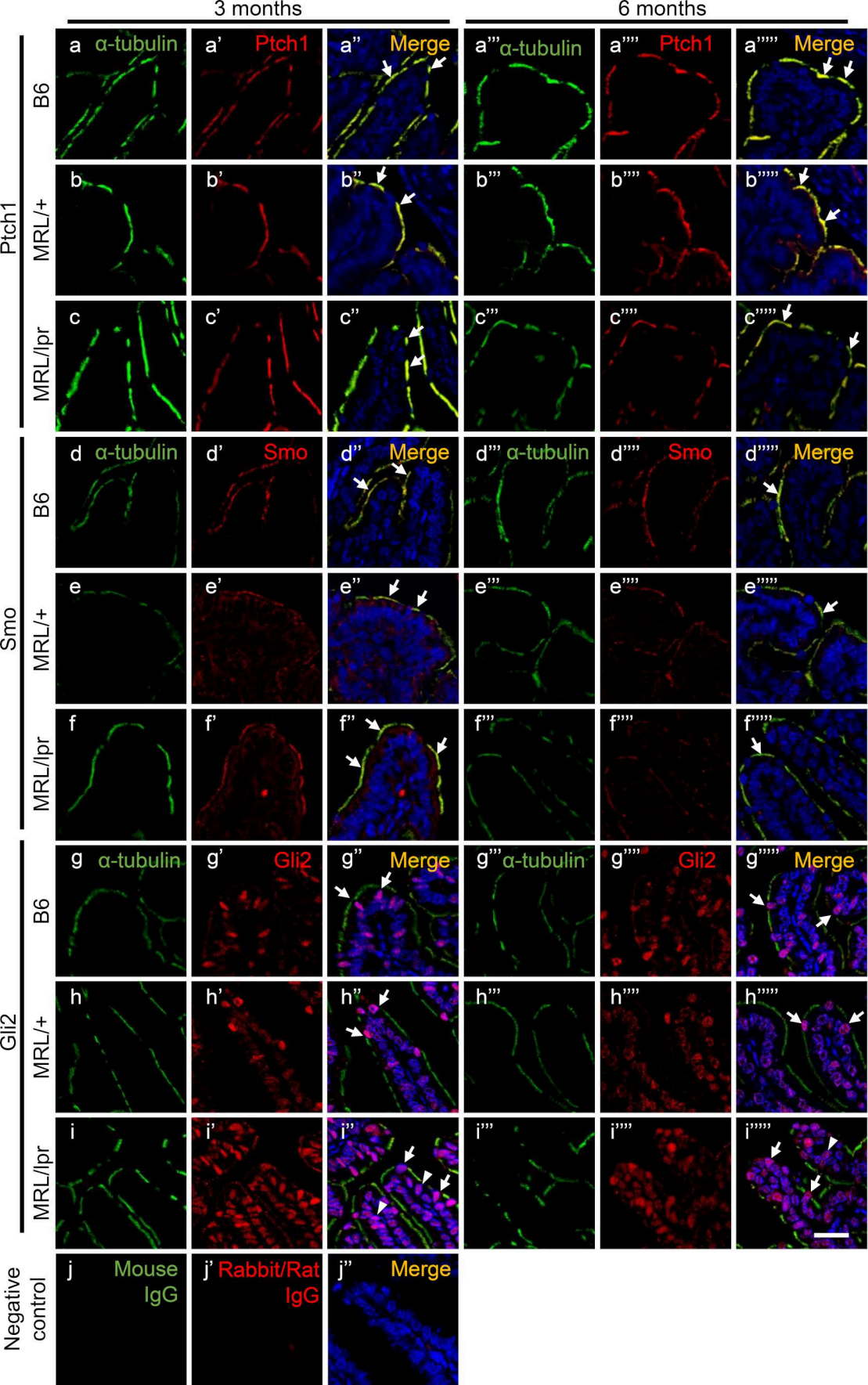
3 months
6 months
Ptch1
Smo
Gli2
Negative control
B6
MRL/+
MRL/lpr
a α-tubulin
a' Ptch1
a'' Merge
a''' α-tubulin
a'''' Ptch1
a''''' Merge
b
b'
b''
b'''
b''''
b'''''
c
c'
c''
c'''
c''''
c'''''
d α-tubulin
d' Smo
d'' Merge
d''' α-tubulin
d'''' Smo
d''''' Merge
e
e'
e''
e'''
e''''
e'''''
f
f'
f''
f'''
f''''
f'''''
g α-tubulin
g' Gli2
g'' Merge
g''' α-tubulin
g'''' Gli2
g''''' Merge
h
h'
h''
h'''
h''''
h'''''
i
i'
i''
i'''
i''''
i'''''
j Mouse IgG
j' Rabbit/Rat IgG
j'' Merge

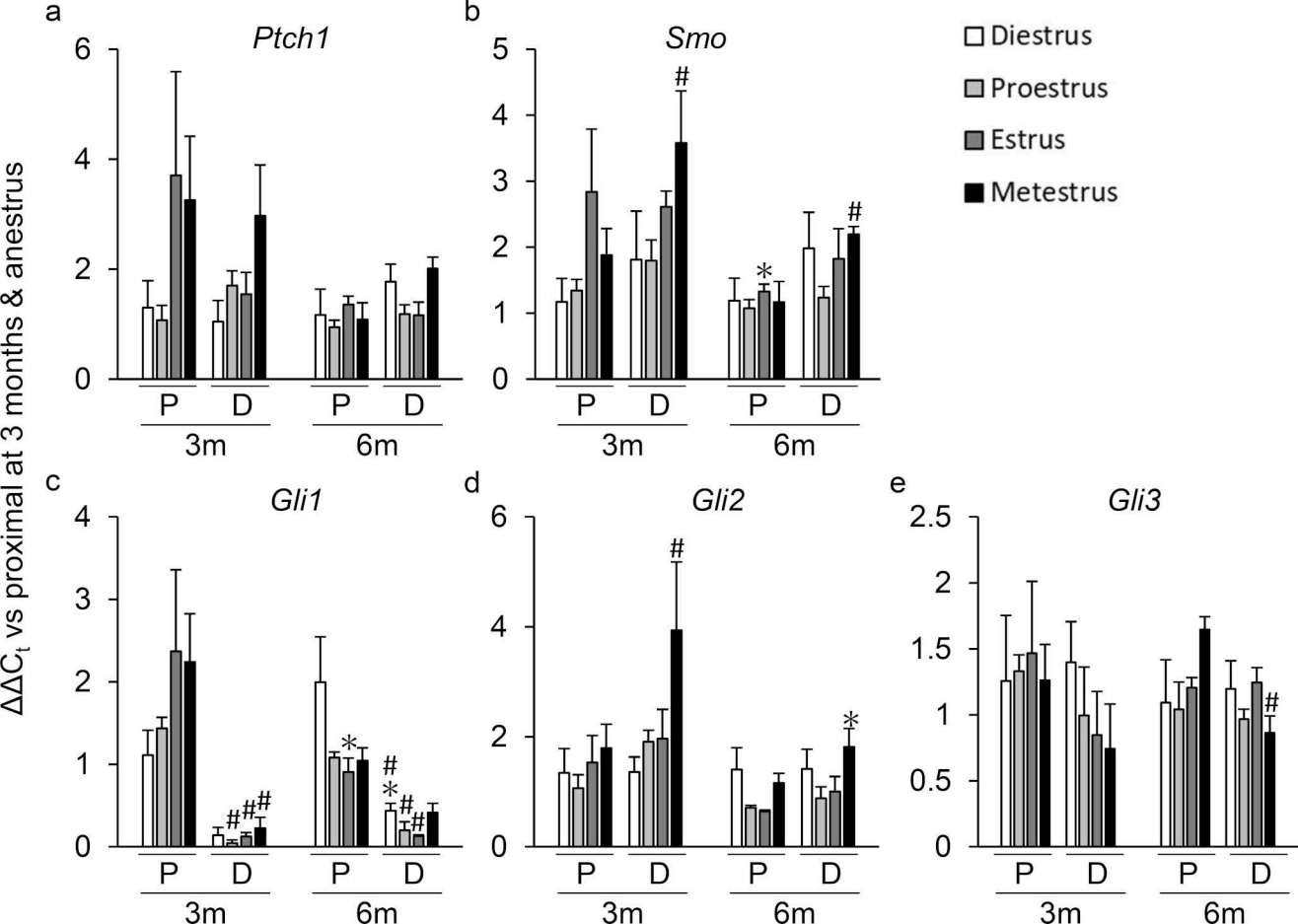
a
Ptch1
b
Smo
c
Gli1
d
Gli2
e
Gli3
Diestrus
Proestrus
Estrus
Metestrus
ΔΔCt vs proximal at 3 months & anestrus
P
D
3m
6m

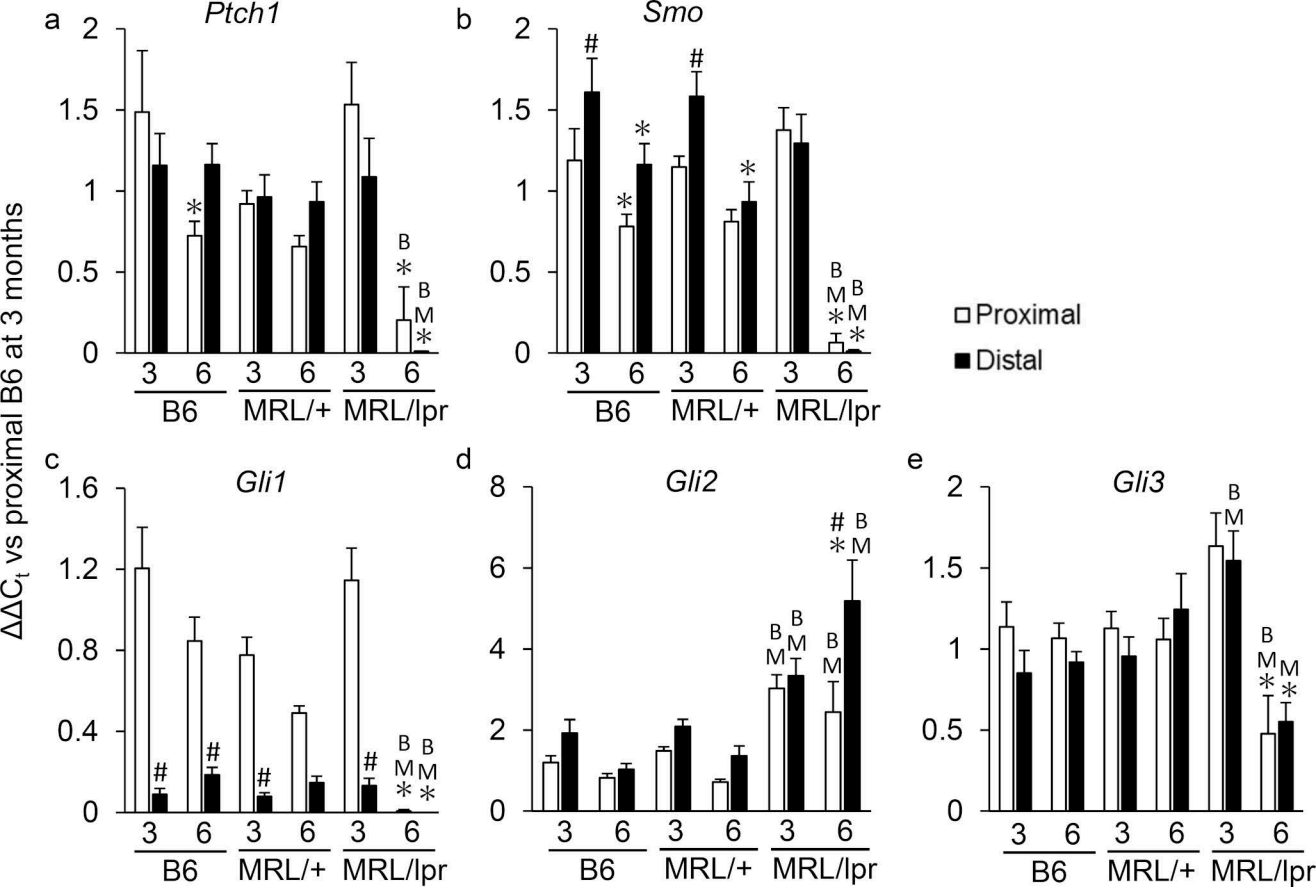
a
Ptch1
b
Smo
c
Gli1
d
Gli2
e
Gli3
ΔΔCt vs proximal B6 at 3 months
Proximal
Distal
3
6
B6
MRL/+
MRL/lpr

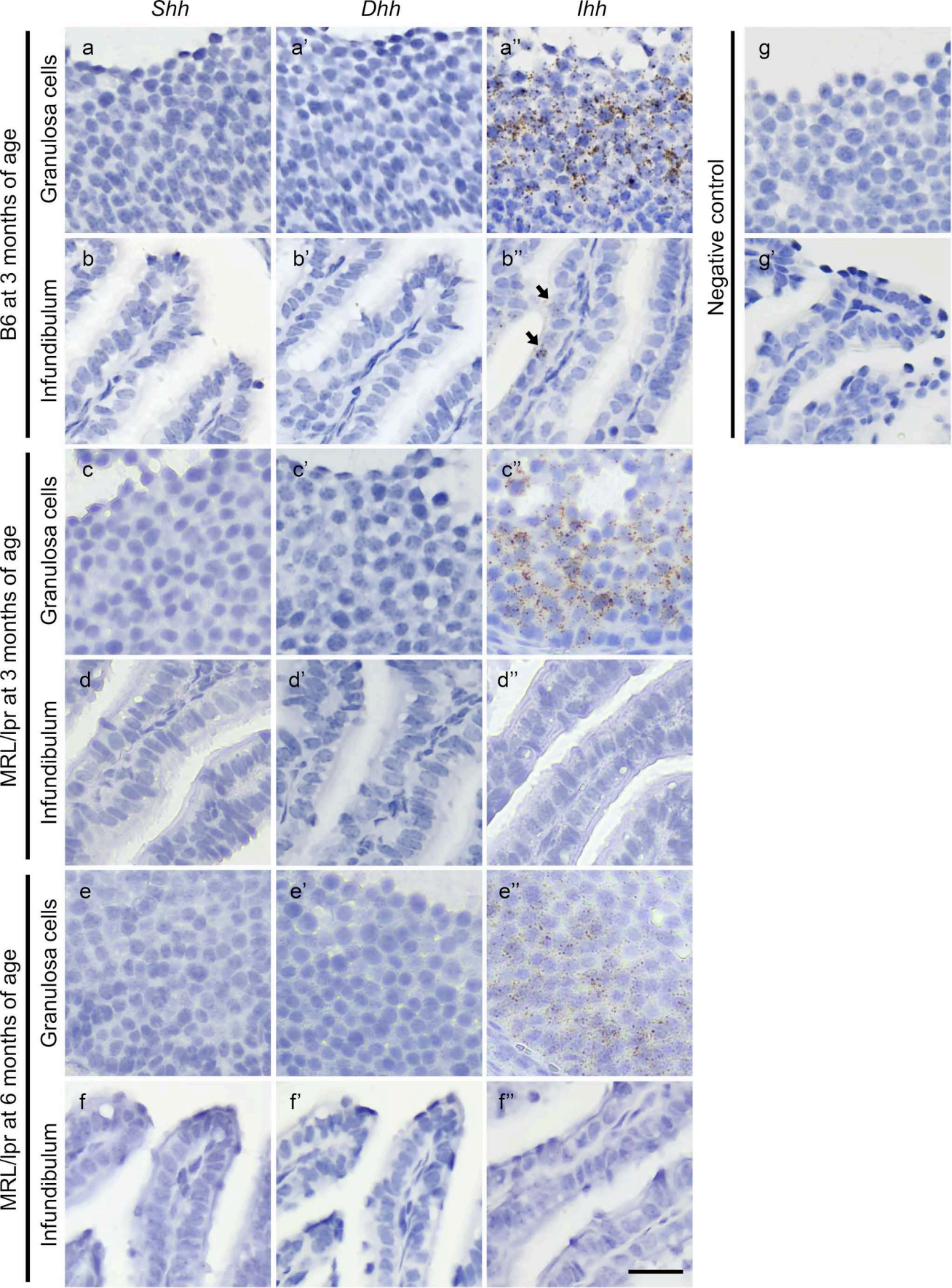
Shh
Dhh
Ihh
B6 at 3 months of age
MRL/lpr at 3 months of age
MRL/lpr at 6 months of age
Granulosa cells
Infundibulum
Negative control
a
a'
a''
b
b'
b''
c
c'
c''
d
d'
d''
e
e'
e''
f
f'
f''
g
g'

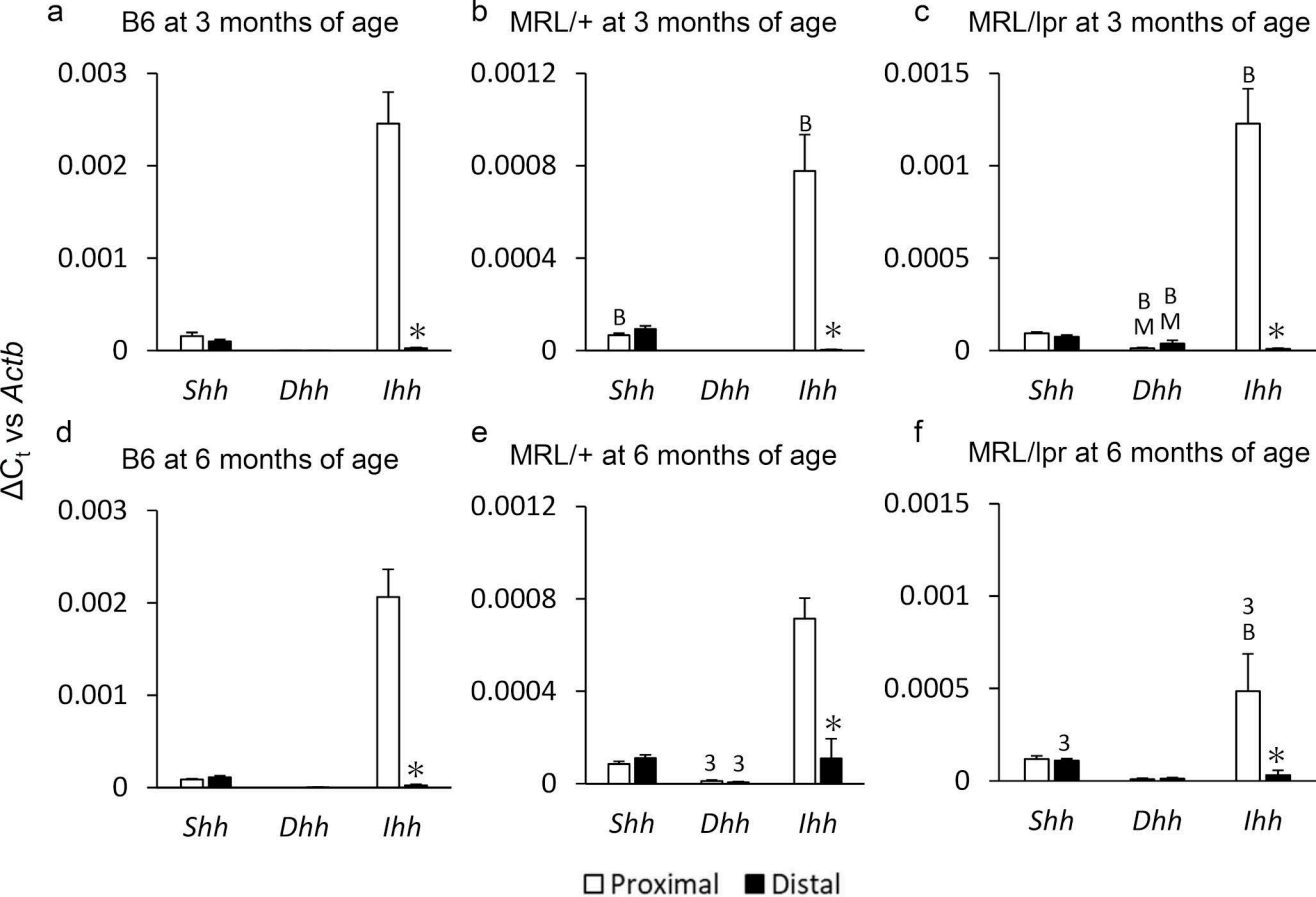
a
B6 at 3 months of age
b
MRL/+ at 3 months of age
c
MRL/lpr at 3 months of age
d
B6 at 6 months of age
e
MRL/+ at 6 months of age
f
MRL/lpr at 6 months of age
ΔCt vs Actb
0.003
0.002
0.001
0
0.0012
0.0008
0.0004
0.0015
0.0005
Shh
Dhh
Ihh
B
M
3
*
Proximal
Distal

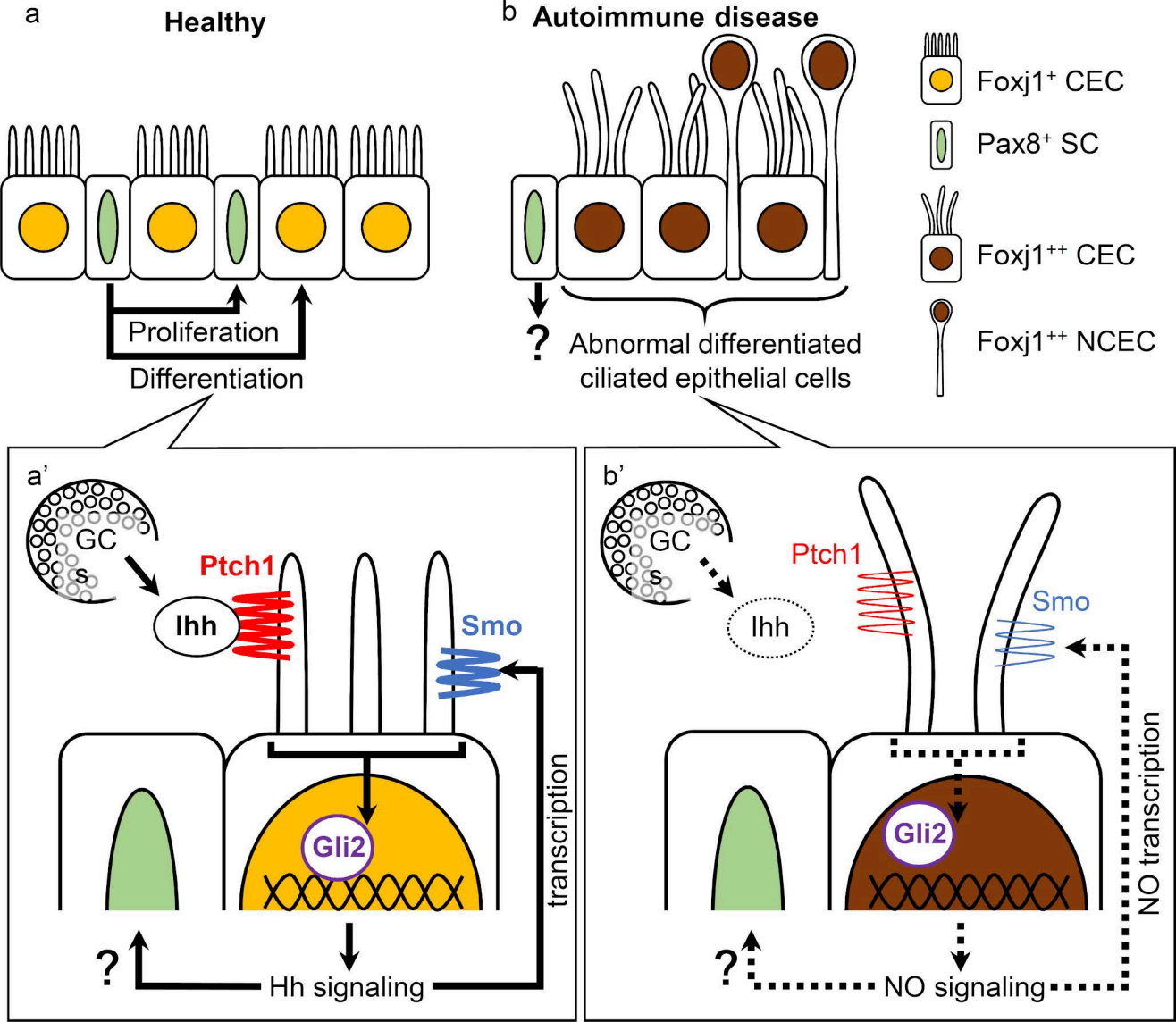
a
Healthy
b
Autoimmune disease
Foxj1+ CEC
Pax8+ SC
Foxj1++ CEC
Foxj1++ NCEC
Proliferation
Differentiation
?
Abnormal differentiated
ciliated epithelial cells
a'
GC
s
Ihh
Ptch1
Smo
Gli2
transcription
?
Hh signaling
b'
GC
s
Ihh
Ptch1
Smo
Gli2
NO transcription
?
NO signaling